



Investigation of Electronic Properties and Dielectric Response of Two-Dimensional Germanium Selenide with Puckered and Buckled Structures

Somayeh Behzad¹ · Raad Chegel²

Received: 15 November 2021 / Accepted: 5 July 2022 / Published online: 22 July 2022
© The Minerals, Metals & Materials Society 2022

Abstract

Utilizing first-principles calculations, the structural, electronic and optical properties of two-dimensional germanium selenide (GeSe) with puckered and buckled structures are investigated. The electronic properties investigations reveal that the buckled GeSe monolayer has an indirect band gap of 2.38 eV and the puckered GeSe monolayer has a direct band gap of 1.15 eV. Applying biaxial strain significantly alters the electronic properties of the puckered and buckled GeSe monolayers. In the buckled GeSe monolayer, the band gap decreases by applying tensile or compressive strain, but for the puckered GeSe monolayer, it becomes zero for -6% strain and increases to 1.49 eV when strain increases to $+6\%$. In the presence of the compressive strain and -6% strain, the puckered GeSe structure shows direct to indirect band gap and semiconductor to metal transitions, respectively. Both materials show a wide range of light absorption covering some part of the visible spectrum.

Keywords Density functional theory · GeSe monolayer · strain · band structure · optical properties

Introduction

Two-dimensional (2D) layered group-IV monochalcogenides MX ($M = \text{Ge}, \text{Sn}$; $X = \text{S}, \text{Se}$) are a newly emerging class of 2D materials which have gained increasing attention and show excellent optoelectronic properties.^{1–6} There are several experimental reports on growth and exfoliation of layered group-IV monochalcogenides such as SnS, GeS and GeSe.^{7–10} 2D layered group-IV monochalcogenides have structures similar to phosphorene. They have superior mechanical flexibility,¹¹ dynamical stability,¹² high thermoelectric performance¹³ and ultralow thermal conductivity,¹⁴ and they are earth abundant with less toxicity than their constituent elements.^{15,16} The phosphorene-like structures also exhibit significant piezoelectric properties with giant piezoelectric coefficients, about two orders of magnitude larger than those of other 2D piezoelectric materials.¹² Because of

their lower structural symmetry with respect to phosphorene, group-IV monochalcogenides are expected to show high ionic dielectric screening¹⁷ and large spin–orbit splitting.³

Another aspect of the superiority of group-IV monochalcogenides over phosphorene is their resistance to oxidation.^{18,19} Phosphorene degrades rapidly under ambient conditions via oxidation, which restricts its future applications.^{20,21} Investigations of the gas-sensing properties of monolayer group-IV monochalcogenides demonstrate that they are potential materials for gas sensors and capturers in future applications.²² Their suitable band gap values,²³ high carrier mobility,²⁴ excellent optical absorption,^{15,25,26} and obvious anisotropic characteristics²⁷ make them promising candidates for applications in optoelectronic and photovoltaic devices.^{2,4,28–30} For instance, by synthesizing the GeSe film with high quality, Xue et al. found that it has a band gap of about 1.14 eV with a high absorption coefficient about 105 cm^{-1} . They also showed that this structure exhibits *p*-type conductivity properties with hole mobility of about $14.85 \text{ cm}^2 \text{ V}^{-1} \text{ s}^{-1}$, which is interesting for thin-film photovoltaic applications.¹⁵ The GeS monolayer has electron mobility of $3680 \text{ cm}^2 \text{ V}^{-1} \text{ s}^{-1}$ which is high compared to structures such as MoS₂ monolayer and silicene field effect transistors.^{24,31} Dai et al. demonstrated that the MX monolayers have high photoresponsivity and external quantum

✉ Somayeh Behzad
somayeh.behzad@gmail.com

¹ Department of Engineering Physics, Kermanshah University of Technology, Kermanshah, Iran

² Physics Department, Faculty of Science, Malayer University, Malayer, Iran

efficiency in the visible region.³⁰ Moreover, these monolayer monochalcogenides show multiferroic properties with ferroelectricity and ferroelasticity properties, and from this category of materials, the GeSe monolayer can retain its properties in a higher temperature region.³² Recently, multilayered GeSe sheets are applied for photovoltaic applications and high-sensitivity photodetector.^{25,33} Also, first-principles calculations showed that a GeSe sheet can be a good candidate for lithium-, sodium- or potassium-ion batteries.^{34,35}

By applying the strain, the electronic properties of the 2D material can be significantly controlled.^{36,37} It has been shown that in-plane strain along the armchair axis can cause a direct–indirect–direct phase transition in phosphorene and the SiS monolayer. Previous studies also showed that by applying biaxial strain, the phase transition from semiconductor to metallic can occur in the GeS monolayer.^{38,39} First-principles study also showed that the ferroelectric polarization of single-layer GeS can be easily modulated via elastic strain engineering.⁴⁰

In this article, the effect of biaxial strain on the electronic and optical properties of hexagonal puckered and buckled GeSe monolayers are investigated by density functional theory (DFT).

Method and Computational Details

In this work, first-principles calculations based on density functional theory (DFT) were performed using the WIEN2K package.³¹ To describe the exchange–correlation interaction, the generalized gradient approximation (GGA) with Perdew–Burke–Ernzerhof (PBE) exchange–correlation functional was used.³² The computational input parameters $R_{\text{MT}} \times K_{\text{max}}$, G_{max} and l_{max} are set to 7, 12 and 10, respectively. For the puckered (buckled) GeSe monolayer, the Brillouin zone is sampled by k-point meshes of $12 \times 13 \times 1$ ($14 \times 14 \times 1$) and $18 \times 20 \times 1$ ($21 \times 21 \times 1$) for electronic structure and optical properties calculations, respectively. The layers are placed in the x – y plane. In the direction perpendicular to the layers, we used vacuum regions of 20 Å between adjacent images to avoid interaction between neighboring images. For the geometry optimizations, the threshold for maximum force was taken as 10^{-3} Ry/a.u.

Results and Discussion

Based on previous research, monolayer GeSe may have two geometrical configurations, namely puckered and buckled structures, similar to phosphorene.^{29,41–43} First, the structural characteristics of puckered and buckled GeSe monolayers are calculated with the structural optimizations. Figures 1 and 2 show the optimized structures of

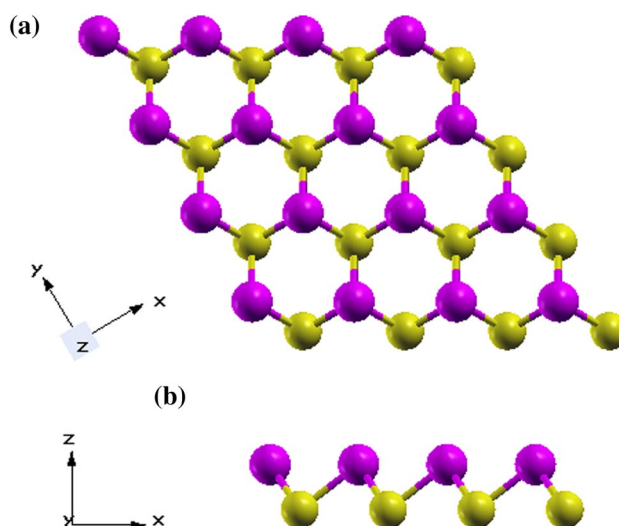


Fig. 1 Optimized structure of GeSe monolayer with buckled structure. (a) Top view of the x – y plane, (b) Side view of the x – z plane.

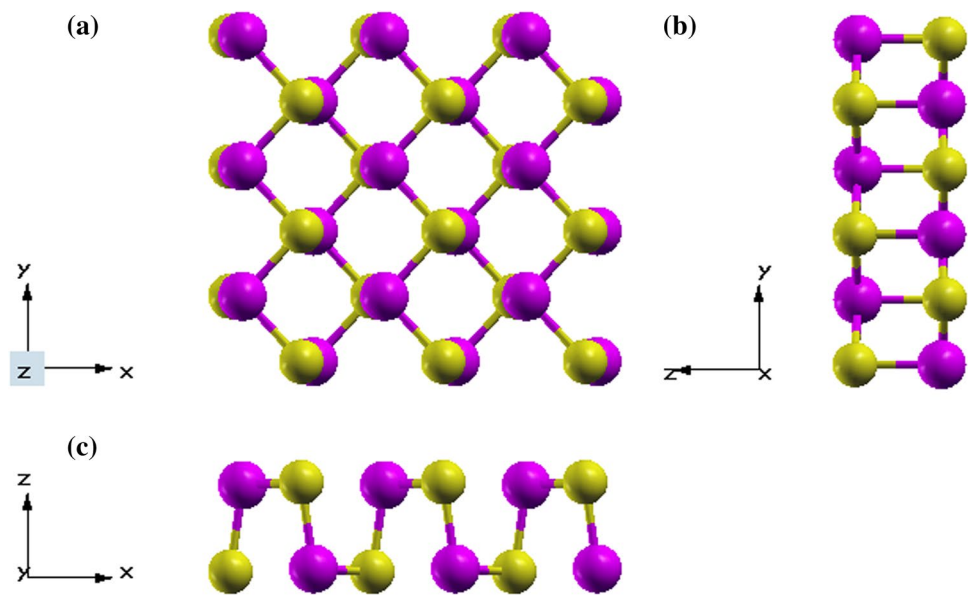
the buckled and puckered GeSe monolayers, respectively. There are two Ge and Se atoms in the hexagonal unit cell of buckled GeSe monolayer, while the rectangular unit cell of puckered GeSe has four atoms (two Ge atoms and two Se atoms) in its unit cell.

Similar to silicene and germanene, in the GeSe monolayer with buckled structure, each Ge (Se) atom is bonded to three neighboring Se (Ge) atoms on other atomic plane forming a hexagonal buckled lattice (see Fig. 1). The optimized buckled GeSe monolayer has lattice constant, buckling height and Ge–Se bond length of 3.67, 1.45 and 2.57 Å, respectively.

As shown in Fig. 2, the puckered GeSe structure has armchair and zigzag configurations along the x and y directions, respectively. Compared to the buckled structure, the puckered GeSe monolayer has rather complicated configuration that reduces the symmetry in this structure. The Ge and Se atoms are bonded together with covalent bonds and each Ge (Se) atom has two neighboring Se (Ge) atoms in the same atomic plane and one Se (Ge) atom in the other atomic plane. The optimized puckered GeSe monolayer has lattice constant parameters $a = 4.29$ Å and $b = 3.97$ Å with in-plane Ge–Se bonds of 2.67 Å and interlayer bridging bonds of 2.54 Å. All obtained optimized parameters are in good accordance with previous reports.^{12,43,44}

Figure 3a, b shows the calculated electronic band structures for buckled and puckered GeSe monolayers, respectively. It can be found that the buckled GeSe monolayer is a semiconductor and it has an indirect band gap of 2.38 eV. The valence band maximum (VBM) is located near the midpoint along the Γ – K direction and the conduction band minimum (CBMs) sites near the M point along the Γ – M direction.

Fig. 2 Optimized structure of GeSe monolayer with puckered structure. (a) Top view of the x - y plane, (b) Side view of the y - z plane. (c) Side view of the x - z plane.



The puckered GeSe monolayer has a direct band gap about 1.15 eV, and in this structure, the VBM and CBM are both located near the X point along the Γ -X direction. The obtained band gaps are in good agreement with previous theoretical results.^{12,29,45}

First, for the buckled and puckered GeSe monolayers, we analyze the contribution of different atomic orbitals to the band structures around the Fermi level. For this purpose, the partial density of states (PDOS) are calculated and the results are given in Fig. 3c, d. The PDOS analysis of the buckled GeSe monolayer indicates that the valence (conduction) bands near the Fermi level mainly originate from the hybridization of Se-4p, Ge-4s and Ge-4p (Se-4p and Ge-4p) orbitals.

The PDOS analysis of the puckered GeSe monolayer indicates that Ge-4p and Se-4p orbitals dominate the electronic states near the Fermi level. The contribution from Ge-4p orbitals to the states of conduction band near the Fermi level is larger than that from Se-4p orbitals, while for the valence band states near the Fermi level, the contribution from Se-4p orbitals is larger than that from Ge-4p and Ge-4s orbitals.

The strain effect is commonly present in 2D materials due to the lattice mismatch between the substrate and 2D materials, or mechanical loading.^{46,47} Also, the band structure of 2D materials has been significantly changed by applying the strain^{46,47} and due to these modifications, the VBM and CBM locations change and the size of the energy gap can be tuned by applying the strain. In this work, the biaxial strain applied on the buckled and puckered GeSe monolayers is calculated from the $\varepsilon = (a - a_0)/a_0 \times 100\%$ expression, where a_0 (a) is the strain-free (strained) lattice constant.

Figures 4 and 5 show the electronic band structure of the buckled and puckered GeSe monolayer in the presence

of the in-plane biaxial strain, with both tensile and compressive strains. When the biaxial tensile strain is applied to the buckled monolayer GeSe, the CBM moves towards the Γ point and it is located at the Γ point for the strains with values greater than 2%. In the presence of the biaxial compressive strain, the CBM and VBM move towards the K and Γ points, respectively and when the compressive strain reaches 4% (1%) and more, the CBM (VBM) is located at the K (Γ) point.

As shown in Fig. 6, in the absence of strain, the band gap of the puckered GeSe monolayer is in its maximum value and it decreases by applying both compressive and tensile strains. Note that, in the presence of the compressive strain, the band gap decreases monotonically with higher decreasing rate. The band gap decreases to 1.04 eV (1.30 eV) when the in-plane strain reaches -8% ($+8\%$).

The puckered GeSe monolayer remains a direct band gap semiconductor under tensile strain up to $+6\%$. The results show that applying the compressive strain induces the direct to indirect gap transition. When the compressive strain becomes -6% , the band gap of the puckered GeSe monolayer closes and a phase transition from semiconductor to metal occurs as shown in Fig. 5. By changing the strain from -6% to $+6\%$, the band gap increases from 0 eV to 1.49 eV (see Fig. 6b).

As shown above, the electronic band structure of the GeSe monolayer is significantly dependent on the strain, and this suggests that applying strain is a simple and effective method for engineering the electronic properties of the GeSe monolayer with puckered and buckled structures, which is useful for future design of 2D devices based on GeSe.

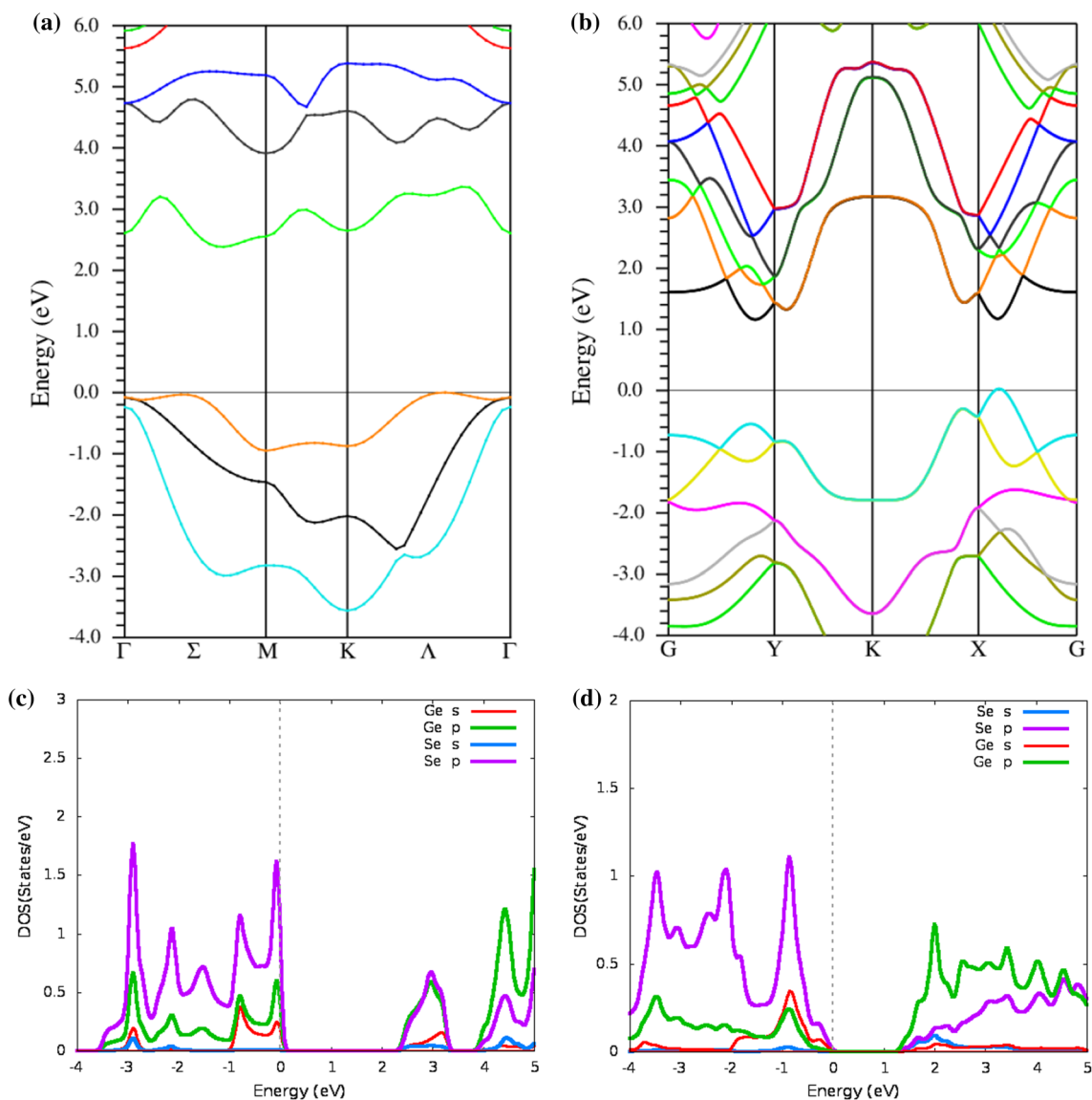


Fig. 3 Electronic band structure for (a) buckled and (b) puckered GeSe monolayers without strain. The partial density of states for (a) buckled and (b) puckered GeSe monolayers.

Optical Properties

The real ($\epsilon_1(\omega)$) and imaginary ($\epsilon_2(\omega)$) parts of the dielectric function, reflectivity ($R(\omega)$) and energy loss function ($L(\omega)$) along three directions for puckered and buckled GeSe monolayers are shown in Figs. 7 and 8, respectively. Because of the structural anisotropy of the puckered GeSe monolayer along the x , y and z directions, the $\epsilon_1(\omega)$, $\epsilon_2(\omega)$, $R(\omega)$ and $L(\omega)$ spectra show different characteristics in the three directions.

For the puckered GeSe monolayer, the first optical absorption peak of $\epsilon_2(\omega)$ along the x , y and z directions occurs at 1.43 eV, 2.24 eV and 4.94 eV, respectively, which means that we can use the puckered GeSe monolayer as a

polarization filter, which blocks or transmits light according to its polarization. The energy region for high absorption along the z direction is larger than that along the x and y directions. The puckered GeSe monolayer exhibits a wide range of light absorption in three light-polarized directions. It shows good absorption efficiency in the visible light region, making it a good candidate for solar cells.

Information about the electronic polarizability can be obtained by investigating the real part of the dielectric function $\epsilon_1(\omega)$ (see Fig. 7b). Accordingly, for the x , y and z directions, we found that the static dielectric constants obtained by $\epsilon_1(0)$, are about 6.41, 6.76 and 3.02, respectively.

By investigation the reflectivity coefficient $R(\omega)$ which is shown in Fig. 7c, the values obtained for the zero-frequency

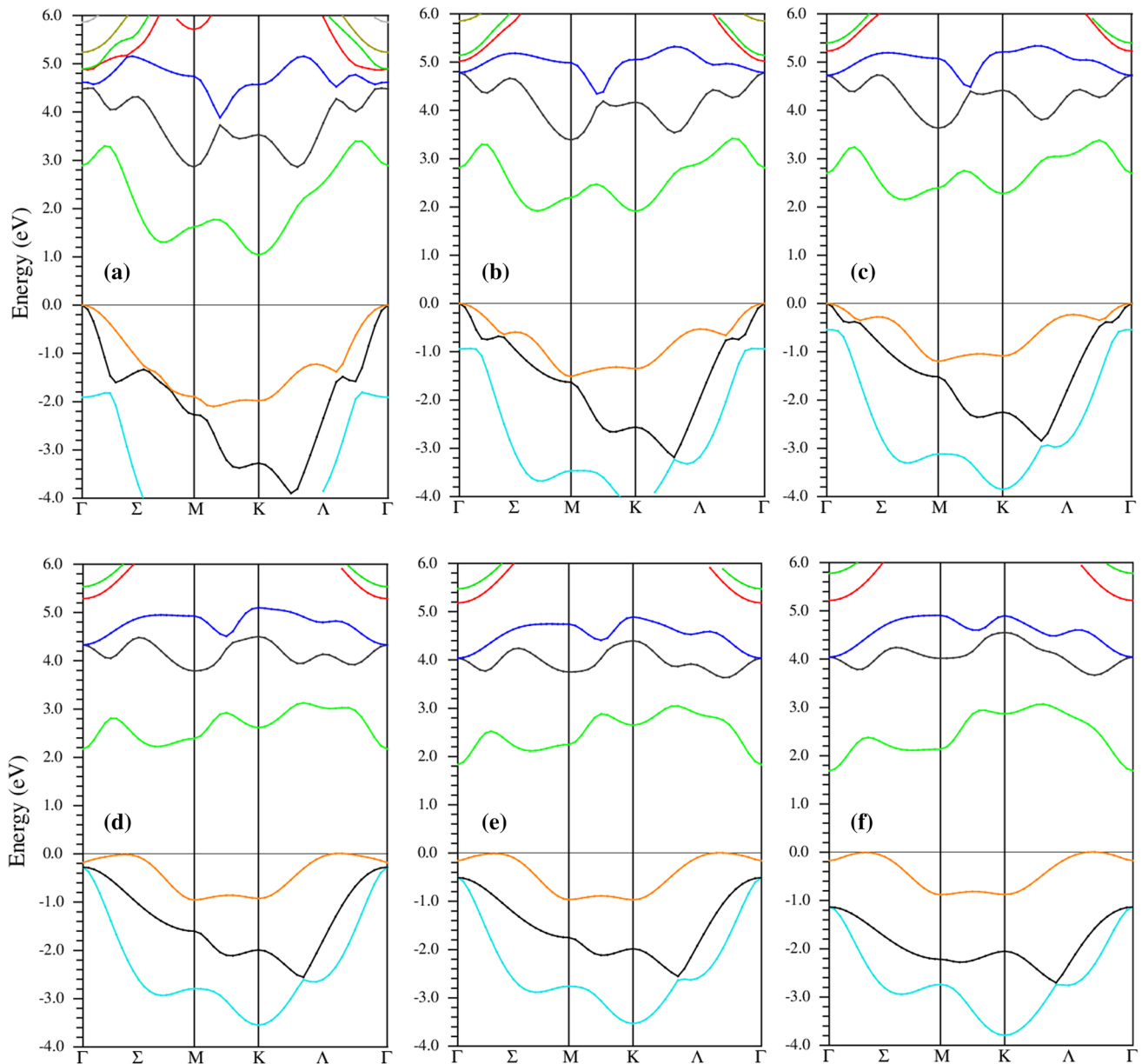


Fig. 4 Electronic band structure of buckled GeSe monolayer under (a) -8% , (b) -4% , (c) -2% , (d) $+2\%$, (e) $+4\%$ and (f) $+8\%$ biaxial strain.

reflectivity $R(0)$ along the x , y and z directions are about 0.19, 0.2, and 0.07, respectively.

The maximum reflectivity values occur at 2.6 eV for Ell_x , 2.54 eV for Ell_y , and 6.16 eV for Ell_z , respectively. The reflectance spectrum shows that at energies with high $\epsilon_2(\omega)$ values, the reflectivity is also high.

The energy loss function $L(\omega)$ (Fig. 7d) is related to the energy loss of a fast electron in the material and is usually large at the plasmon energy. The $L(\omega)$ spectrum has prominent peaks at energies about 10.08 eV, 10.25 eV and 11.01 eV for Ell_x , Ell_y and Ell_z polarizations, respectively, and these peaks are related to the plasmon resonance.

For the buckled GeSe monolayer, the optical spectra are degenerate along the x and y directions, due to hexagonal symmetry of the structure. From Fig. 8a, for the imaginary part $\epsilon_2(\omega)$, it can be observed that the first absorption peak along the x and z directions occurs at 3.5 eV and 3.22 eV, respectively. The absorption edge lies in the visible light region. For Ell_z , most of the absorption occurs in the ultraviolet light region.

The static dielectric constant $\epsilon_1(0)$ along the x and z directions is found to be 3.3 and 2.27, respectively (see Fig. 8b). The zero-frequency reflectivity $R(0)$ (maximum reflectivity value) along the x and z directions is 0.08 (6.00) and 0.04

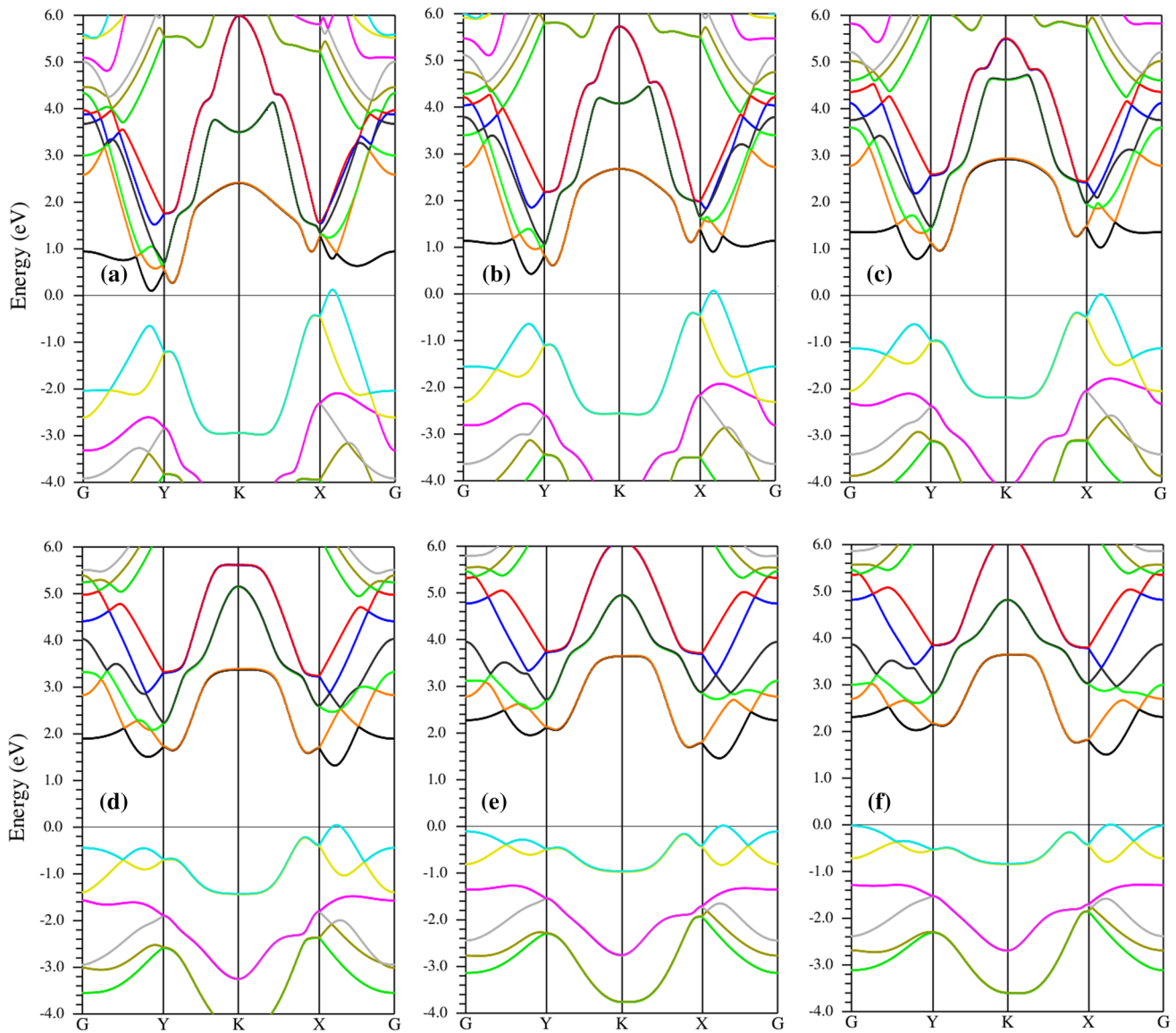


Fig. 5 Electronic band structure of puckered GeSe monolayer under (a) -6% , (b) -4% , (c) -2% , (d) $+2\%$, (e) $+4\%$ and (f) $+6\%$ biaxial strain.

Fig. 6 The evolution of band gap for (a) buckled and (b) puckered GeSe monolayers as a function of the applied strain.

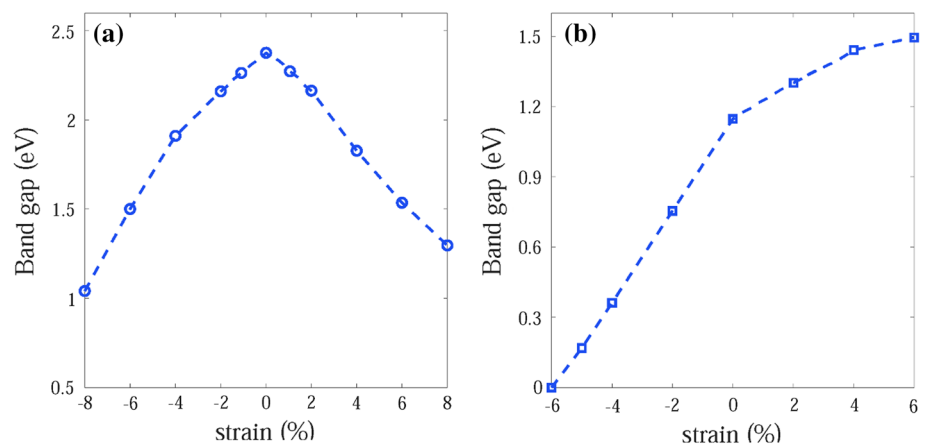


Fig. 7 Calculated optical spectra including the (a) imaginary $\epsilon_2(\omega)$ and (b) real $\epsilon_1(\omega)$ parts of the dielectric function, (c) reflectivity $R(\omega)$ and (d) energy loss function $L(\omega)$ in x , y and z directions for the puckered GeSe monolayer.

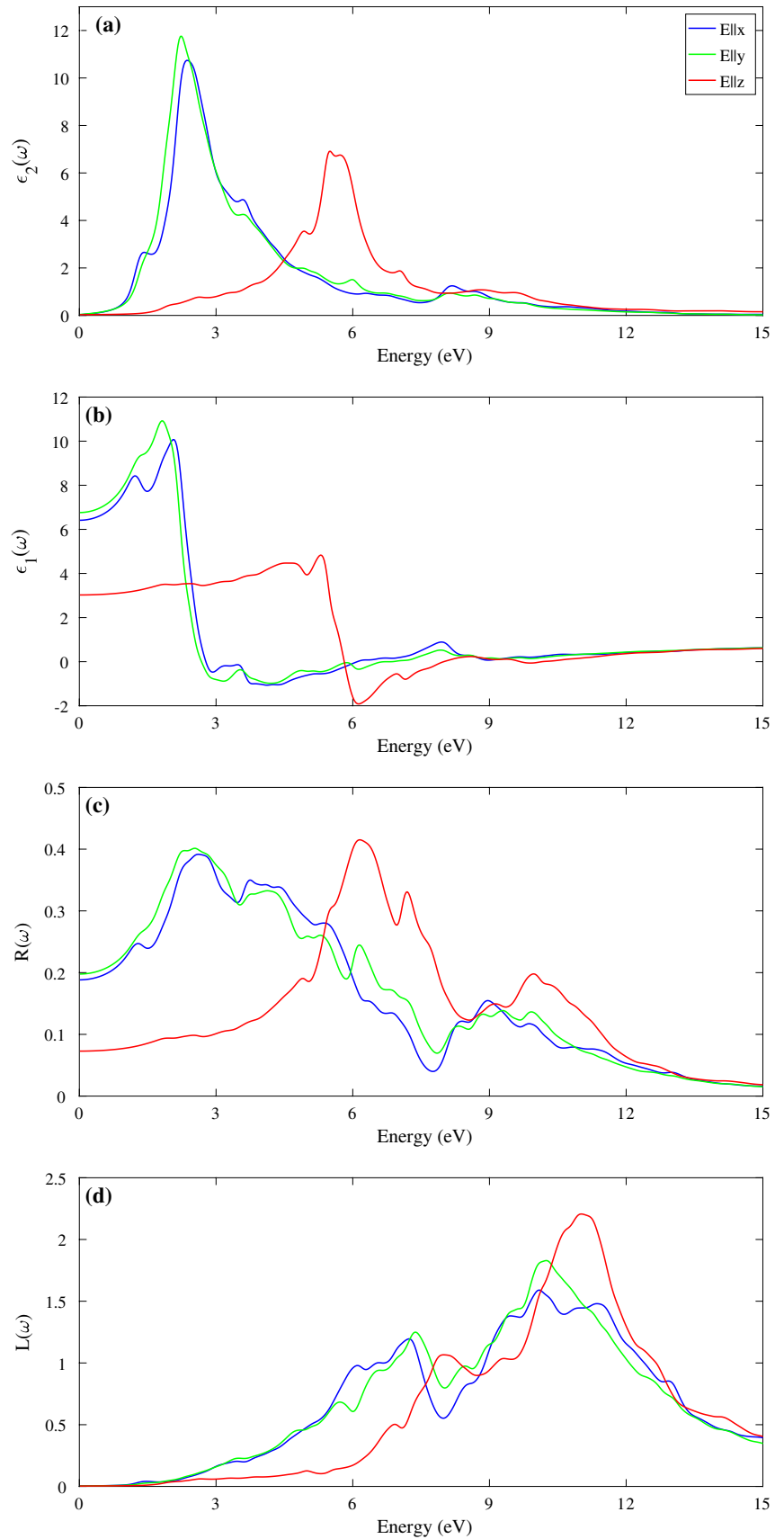


Fig. 8 Calculated optical spectra including the (a) imaginary $\epsilon_2(\omega)$ and (b) real $\epsilon_1(\omega)$ parts of the dielectric function, (c) reflectivity $R(\omega)$ and (d) energy loss function $L(\omega)$ in x and z directions for the buckled GeSe monolayer.

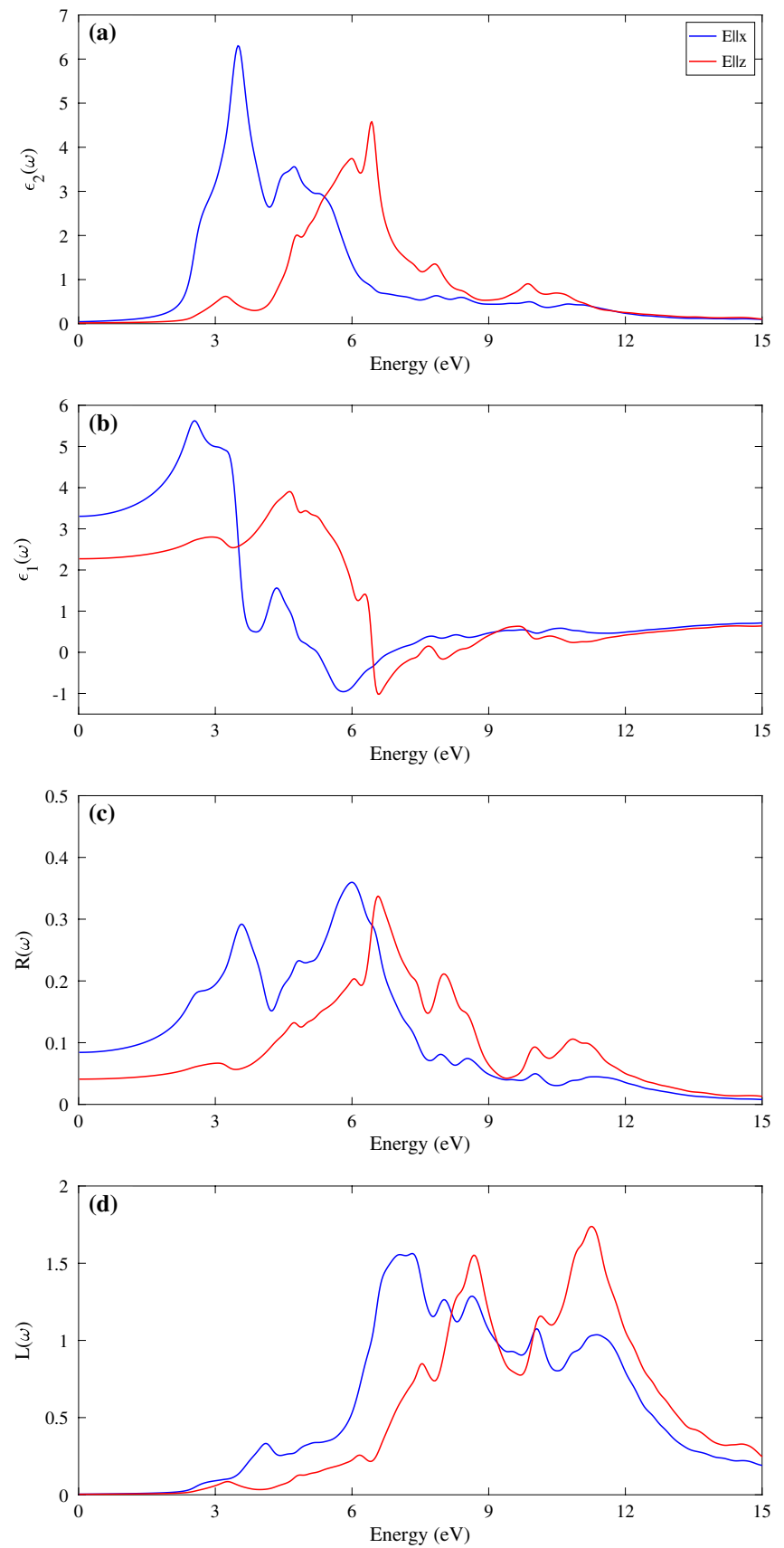


Fig. 9 Imaginary $\epsilon_2(\omega)$ part of the dielectric function for the puckered GeSe monolayer under different applied strain along the x direction.

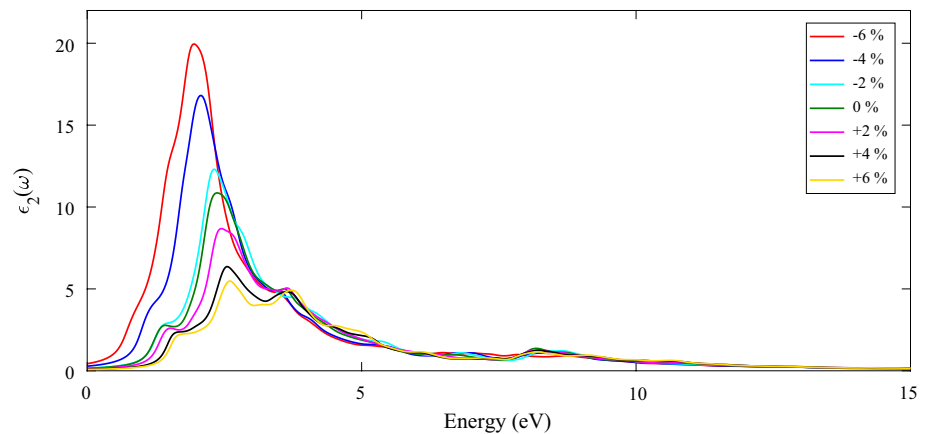
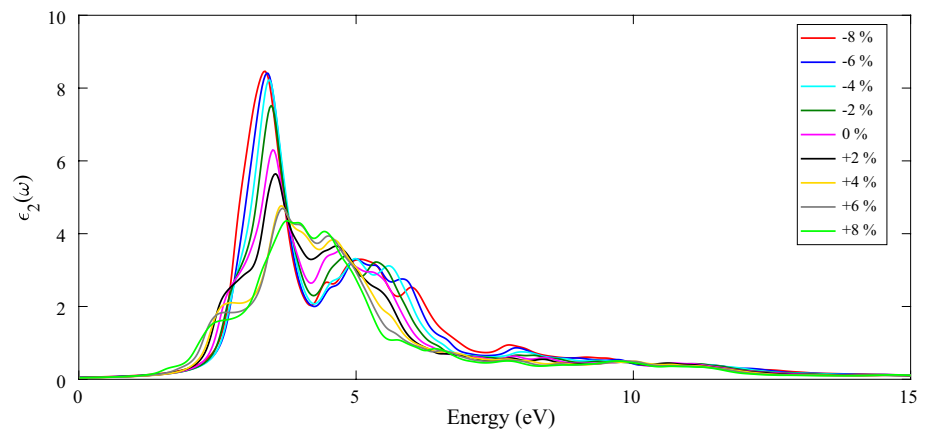


Fig. 10 Imaginary $\epsilon_2(\omega)$ part of the dielectric function for the buckled GeSe monolayer under different applied strain along the x direction.



(6.57), respectively. The most prominent peak in $L(\omega)$ is at 0.25 eV and 11.01 eV for $E_{||x}$ and $E_{||z}$ polarization. In Figs. 9 and 10, we report calculations of $\epsilon_2(\omega)$ for puckered and buckled GeSe monolayers under different applied strain along the x direction. As shown in Figs. 9 and 10, the intensity of main absorption peak of puckered and buckled GeSe monolayers along the x direction decreases and shifts to higher energies as the strain changes from -6% to $+6\%$. For buckled structure, the first absorption peak disappears by applying compressive strain and it shifts to higher energies by applying tensile strain. For puckered structure, the absorption edge shifts to lower energies by increasing the tensile strain. Therefore, the width of the adsorption area can be tuned by applying strain.

Conclusion

Here, we investigated the in-plane biaxial strain effects on the electronic and optical properties of puckered and buckled GeSe monolayers by DFT computations. The buckled GeSe monolayer remains an indirect gap semiconductor under biaxial strain and its band can be reduced to 1.04 eV (1.30 eV) by applying a biaxial strain of -8% ($+8\%$). For the puckered GeSe monolayer, the semiconductor to metal transition and direct to indirect gap transition occur at certain values of the biaxial strain.

The optical spectrum of the puckered GeSe monolayer shows anisotropy along the x , y and z directions, due to the structural anisotropy, while that of the buckled GeSe monolayer is degenerate along the x and y directions. The puckered GeSe monolayer shows good absorption efficiency in the visible light region, making it a good candidate for solar cells.

References

- Z. Hu, Y. Ding, X. Hu, W. Zhou, X. Yu, and S. Zhang, Recent Progress in 2D Group IV–IV Monochalcogenides: Synthesis, Properties and Applications. *Nanotechnology* 30, 252001 (2019).
- C. Chowdhury, S. Karmakar, and A. Datta, Monolayer Group IV–VI Monochalcogenides: Low-Dimensional Materials for Photocatalytic Water Splitting. *J. Phys. Chem. C* 121, 7615–7624 (2017).
- L.C. Gomes and A. Carvalho, Phosphorene Analogues: Isoelectronic Two-dimensional Group-IV Monochalcogenides with Orthorhombic Structure. *Phys. Rev. B* 92, 085406 (2015).
- S.R. Tamalampudi, S. Patole, B. Alfakes, R. Sankar, I. Alman-souri, M. Chiesa, and J.-Y. Lu, High-Temperature Defect-Induced Hopping Conduction in Multilayered Germanium Sulfide for Optoelectronic Applications in Harsh Environments. *ACS Appl. Nano Mater.* 2, 2169–2175 (2019).
- D. Tan, H.E. Lim, F. Wang, N.B. Mohamed, S. Mouri, W. Zhang, Y. Miyauchi, M. Ohfuchi, and K. Matsuda, Anisotropic Optical and Electronic Properties of Two-Dimensional Layered Germanium Sulfide. *Nano Res.* 10, 546–555 (2017).
- A.K. Tołłoczko, S.J. Zelewski, M. Błaszczak, T. Woźniak, A. Siudzińska, A. Bachmatiuk, P. Scharoch, and R. Kudrawiec, Optical Properties of Orthorhombic Germanium Selenide: An Anisotropic Layered Semiconductor Promising for Optoelectronic Applications. *J. Mater. Chem. C* (2021). <https://doi.org/10.1039/D1TC04280G>.
- B. Mukherjee, Y. Cai, H.R. Tan, Y.P. Feng, E.S. Tok, and C.H. Sow, NIR Schottky Photodetectors Based on Individual Single-Crystalline GeSe Nanosheet. *ACS Appl. Mater. Interfaces.* 5, 9594–9604 (2013).
- C. Li, L. Huang, G.P. Snigdha, Y. Yu, and L. Cao, Role of Boundary Layer Diffusion in Vapor Deposition Growth of Chalcogenide Nanosheets: The Case of GeS. *ACS Nano* 6, 8868–8877 (2012).
- J.R. Brent, D.J. Lewis, T. Lorenz, E.A. Lewis, N. Savjani, S.J. Haigh, G. Seifert, B. Derby, and P. O'Brien, Tin(II) Sulfide (SnS) Nanosheets by Liquid-Phase Exfoliation of Herzenbergite: IV–VI Main Group Two-Dimensional Atomic Crystals. *J. Am. Chem. Soc.* 137, 12689–12696 (2015).
- D.-J. Xue, J. Tan, J.-S. Hu, W. Hu, Y.-G. Guo, and L.-J. Wan, Anisotropic Photoresponse Properties of Single Micrometer-Sized GeSe Nanosheet. *Adv. Mater.* 24, 4528–4533 (2012).
- Y. Gao, L. Zhang, G. Yao, and H. Wang, Unique Mechanical Responses of Layered Phosphorus-Like Group-IV Monochalcogenides. *J. Appl. Phys.* 125, 082519 (2019).
- T. Hu and J. Dong, Two New Phases of Monolayer Group-IV Monochalcogenides and Their Piezoelectric Properties. *Phys. Chem. Chem. Phys.* 18, 32514–32520 (2016).
- F.Q. Wang, S. Zhang, J. Yu, and Q. Wang, Thermoelectric Properties of Single-Layered SnSe Sheet. *Nanoscale* 7, 15962–15970 (2015).
- P.-F. Liu, T. Bo, J. Xu, W. Yin, J. Zhang, F. Wang, O. Eriksson, and B.-T. Wang, First-Principles Calculations of the Ultralow Thermal Conductivity in Two-Dimensional Group-IV Selenides. *Phys. Rev. B* 98, 235426 (2018).
- D.-J. Xue, S.-C. Liu, C.-M. Dai, S. Chen, C. He, L. Zhao, J.-S. Hu, and L.-J. Wan, GeSe Thin-Film Solar Cells Fabricated by Self-Regulated Rapid Thermal Sublimation. *J. Am. Chem. Soc.* 139, 958–965 (2017).
- X. Song, W. Zhou, X. Liu, Y. Gu, and S. Zhang, Layer-Controlled Band Alignment, Work Function and Optical Properties of Few-Layer GeSe. *Physica B* 519, 90–94 (2017).
- L.C. Gomes, A. Carvalho, and A.H. Castro Neto, Enhanced Piezoelectricity and Modified Dielectric Screening of Two-Dimensional Group-IV Monochalcogenides. *Phys. Rev. B* 92, 214103 (2015).
- Y. Guo, S. Zhou, Y. Bai, and J. Zhao, Oxidation Resistance of Monolayer Group-IV Monochalcogenides. *ACS Appl. Mater. Interfaces.* 9, 12013–12020 (2017).
- L.C. Gomes, A. Carvalho, and A.H. Castro Neto, Vacancies and Oxidation of Two-Dimensional Group-IV Monochalcogenides. *Physical Review B* 94, 054103 (2016).
- G. Wang, W.J. Slough, R. Pandey, and S.P. Karna, Degradation of Phosphorene in Air: Understanding at Atomic Level. *2D Materials* 3, 025011 (2016).
- A. Ziletti, A. Carvalho, P.E. Trevisanutto, D.K. Campbell, D.F. Coker, and A.H. Castro Neto, Phosphorene Oxides: Bandgap Engineering of Phosphorene by Oxidation. *Phys. Rev. B* 91, 085407 (2015).
- S. Ma, D. Yuan, Y. Wang, and Z. Jiao, Monolayer GeS as a Potential Candidate for NO₂ Gas Sensors and Capturers. *J. Mater. Chem. C* 6, 8082–8091 (2018).
- L. Xu, M. Yang, S.J. Wang, and Y.P. Feng, Electronic and Optical Properties of the Monolayer Group-IV Monochalcogenides M X (M = Ge, Sn; X = S, Se, Te). *Phys. Rev. B* 95, 235434 (2017).
- F. Li, X. Liu, Y. Wang, and Y. Li, Germanium Monosulfide Monolayer: A Novel Two-Dimensional Semiconductor with a High Carrier Mobility. *J. Mater. Chem. C* 4, 2155–2159 (2016).
- S.-C. Liu, Y. Mi, D.-J. Xue, Y.-X. Chen, C. He, X. Liu, J.-S. Hu, and L.-J. Wan, Investigation of Physical and Electronic Properties of GeSe for Photovoltaic Applications. *Adv. Electron. Mater.* 3, 1700141 (2017).
- C. Xia, J. Du, W. Xiong, Y. Jia, Z. Wei, and J. Li, A Type-II GeSe/SnS Heterobilayer with a Suitable Direct Gap, Superior Optical Absorption and Broad Spectrum for Photovoltaic Applications. *J. Mater. Chem. A* 5, 13400–13410 (2017).
- P. Sutter and E. Sutter, Growth Mechanisms of Anisotropic Layered Group IV Chalcogenides on van der Waals Substrates for Energy Conversion Applications. *ACS Appl. Nano Mater.* 1, 3026–3034 (2018).
- D. Gu, X. Tao, H. Chen, W. Zhu, Y. Ouyang, and Q. Peng, Enhanced Photocatalytic Activity for Water Splitting of Blue-Phase GeS and GeSe Monolayers Via Biaxial Straining. *Nanoscale* 11, 2335–2342 (2019).
- Y. Ji, M. Yang, H. Dong, T. Hou, L. Wang, and Y. Li, Two-Dimensional Germanium Monochalcogenide Photocatalyst for Water Splitting Under Ultraviolet, Visible to Near-Infrared Light. *Nanoscale* 9, 8608–8615 (2017).
- P. Zhao, H. Yang, J. Li, H. Jin, W. Wei, L. Yu, B. Huang, and Y. Dai, Design of New Photovoltaic Systems Based on Two-Dimensional Group-IV Monochalcogenides for High Performance Solar Cells. *J. Mater. Chem. A* 5, 24145–24152 (2017).
- T.P. Kaloni, G. Schreckenbach, M.S. Freund, and U. Schwingenschlögl, Current developments in silicene and germanene. *Physica Status Solidi (RRL) Rapid Res. Lett.* 10, 133–142 (2016).
- M. Wu and X.C. Zeng, Intrinsic Ferroelasticity and/or Multiferroicity in Two-Dimensional Phosphorene and Phosphorene Analogues. *Nano Lett.* 16, 3236–3241 (2016).
- P. Ramasamy, D. Kwak, D.-H. Lim, H.-S. Ra, and J.-S. Lee, Solution Synthesis of GeS and GeSe Nanosheets for High-Sensitivity Photodetectors. *J. Mater. Chem. C* 4, 479–485 (2016).
- Y. Zhou, MX (M = Ge, Sn; X = S, Se) Sheets: Theoretical Prediction of New Promising Electrode Materials for Li Ion Batteries. *J. Mater. Chem. A* 4, 10906–10913 (2016).
- A. Sannyal, Z. Zhang, X. Gao, and J. Jang, Two-Dimensional Sheet of Germanium Selenide as an Anode Material for Sodium and Potassium Ion Batteries: First-Principles Simulation Study. *Comput. Mater. Sci.* 154, 204–211 (2018).
- S. Behzad, Strain-Induced Band Gap Tuning in α -Graphyne on Its Boron Nitride Analog Substrate. *Eur. Phys. J. B* 92, 7 (2019).

37. S. Behzad, Strain Engineering of Band Dispersion and Dielectric Response of Monolayer and Bilayer AlN. *J. Comput. Electron.* 17, 514–520 (2018).
38. S. Zhang, N. Wang, S. Liu, S. Huang, W. Zhou, B. Cai, M. Xie, Q. Yang, X. Chen, and H. Zeng, Two-Dimensional GeS with Tunable Electronic Properties via External Electric Field and Strain. *Nanotechnology* 27, 274001 (2016).
39. L. Huang, F. Wu, and J. Li, Structural Anisotropy Results in Strain-Tunable Electronic and Optical Properties in Monolayer GeX and SnX (X = S, Se, Te). *J. Chem. Phys.* 144, 114708 (2016).
40. H. Wang and X. Qian, Two-dimensional multiferroics in monolayer group IV monochalcogenides. *2D Materials* 4, 015042 (2017).
41. Y.-L. Zhu, Y. Junhui, Y.-Q. Song, S. Wang, K.-H. Xue, M. Xu, X.-M. Cheng, X.-S. Miao, Two-Dimensional Silicon Chalcogenides with High Carrier Mobility for Photocatalytic Water Splitting. *J. Mater. Sci.* 54 (2019).
42. H.R. Jiang, T.S. Zhao, M. Liu, M.C. Wu, and X.H. Yan, Two-Dimensional SiS as a Potential Anode Material for Lithium-Based Batteries: A First-Principles Study. *J. Power Sources* 331, 391–399 (2016).
43. C. Kamal, A. Chakrabarti, and M. Ezawa, Direct Band Gaps in Group IV–VI Monolayer Materials: Binary Counterparts of Phosphorene. *Phys. Rev. B* 93, 125428 (2016).
44. J. Yujin, M. Yang, H. Dong, T. Hou, L. Wang, Y. Li, Two-Dimensional Germanium Monochalcogenide Photocatalyst for Water Splitting under Ultraviolet, Visible to Near-infrared Light. *Nanoscale*, 9 (2017).
45. Y. Xu, K. Xu, H. Zhang, First-Principles Calculations of Angular and Strain Dependence on Effective Masses of Two-Dimensional Phosphorene Analogues (Monolayer α -Phase Group-IV Monochalcogenides MX), *Molecules* (Basel, Switzerland), 2019.
46. K.S. Novoselov and A.H. Castro Neto, Two-Dimensional Crystals-Based Heterostructures: Materials with Tailored Properties. *Physica Scripta* T146, 014006 (2012).
47. M. Ghorbani-Asl, S. Borini, A. Kuc, and T. Heine, Strain-Dependent Modulation of Conductivity in Single Layer Transition-Metal Dichalcogenides. *Phys. Rev. B* 87, 235434 (2013).

Publisher's Note Springer Nature remains neutral with regard to jurisdictional claims in published maps and institutional affiliations.